JOURNAL OF THEORETICAL AND APPLIED MECHANICS
46, 3, pp. 621-640, Warsaw 2008

EXPERIMENTAL AND NUMERICAL STUDIES OF INCLINED CABLES: FREE AND PARAMETRICALLY-FORCED VIBRATIONS

Giuseppe Rega
SAPIENZA University of Rome, Department of Structural and Geotechnical Engineering, Italy
e-mail: giuseppe.rega@uniroma1.it

Narakorn Srinil
University of Aberdeen, King's College, Centre for Applied Dynamics Research, Department of Engineering, Scotland, UK; e-mail: narakorn.srinil@abdn.ac.uk

Rocco Alaggio
University of L'Aquila, Department of Structures, Water and Soil Engineering, Italy
e-mail: ala@ing.univaq.it

Because of few experimental studies in the inclined cable literature, this paper is aimed at experimental modelling and investigating the linear free and nonlinear forced vibrations of sagged inclined cables, by discussing the relevant outcomes in the background of theoretical and numerical achievements. Attention is paid to the identification of cable hybrid modes due to system asymmetry, which gives rise to an avoidance phenomenon in the natural frequency spectrum, and to the investigation of some typical 3-D nonlinear dynamics involving the simultaneous parametric/external excitation due to a harmonically time-varying support movement. Large-amplitude out-of-plane/in-plane multi-modal interactions due to non-planar/planar internal resonances are experimentally observed and complemented by space-time numerical simulation of the associated, geometrically nonlinear, partial-differential equations of parametrically-forced cable motion. Overall, the experimental and numerical results highlight the fundamental linear/nonlinear dynamic characteristics of inclined cables, and the crucial role played by the asymmetry induced by cable inclination, in addition to the significant effects of cable sag and dynamic extensibility.

Key words: inclined cable, frequency avoidance, hybrid modes, parametric resonance, experimental dynamics, numerical simulation

1. Introduction

Linear and nonlinear dynamics of elastic suspended cables have attracted considerable research effort in the last few decades owing to their intrinsic the-

oretical interest and to a large variety of practical applications. Relevant basic knowledge in the linear range is summarized in the classical book by Irvine (1981) and in some review articles by Triantafyllou (1984, 1987, 1991), whereas nonlinear modelling, analysis and phenomena are comprehensively addressed in the recent review papers by Rega (2004) and Ibrahim (2004) concerned with deterministic and stochastic dynamics, respectively.

Besides a large amount of theoretical investigations, experimental analyses have also been carried out in the recent literature, with the aim of enriching the understanding of diverse linear (e.g., Lee and Perkins, 1993; Cheng and Perkins, 1994) and nonlinear (Rega *et al.*, 1997; Benedettini and Rega, 1997; Alaggio and Rega, 2000) dynamic characteristics of cables against the analytical-numerical outcomes. Yet, experimental investigations have mostly dealt with sagged horizontal cables or nearly-taut inclined cables, whose static configurations are theoretically, as well as experimentally, symmetric, albeit being inclined. On the contrary, few experimental studies (Russell and Lardner, 1998; Xu *et al.*, 1999) have been reported on sagged inclined cables which, due to actually asymmetric inclined configurations, exhibit in the linear range the so-called frequency avoidance (veering) phenomenon (Triantafyllou and Grinfogel, 1986) – with the coexisting *hybrid* (i.e., mixed symmetric/anti-symmetric) modes – instead of the classic frequency crossover phenomenon – with the coexisting *purely* symmetric/anti-symmetric modes – characteristic for sagged horizontal cables (Irvine and Caughey, 1974). Therefore, it seems worth (i) ascertaining, through experiments, the actual occurrence of such frequency avoidance and of the corresponding hybrid modes, and (ii) highlighting the influence of system asymmetry on cable nonlinear dynamics involving multi-modal in-plane/out-of-plane resonant interactions, with (iii) the latter issue being investigated also in the background of numerical results furnished by a systematic theoretical approach accounting for full 3-D mechanics and high-dimensional system discretization (Srinil *et al.*, 2007; Srinil and Rega, 2007b, 2008).

Accordingly, in this paper, the experimental 3-D dynamics of an extensible sagged inclined cable subject to harmonically time-varying support motion in the horizontal direction is investigated. A similar problem was addressed, e.g., in Perkins (1992) and in Koh and Rong (2004), yet considering a horizontal cable. Based on a reduced two degree-of-freedom model, Perkins (1992) showed a qualitative agreement between analytical and experimental results in the case of varying amplitude of the support motion leading to a non-planar 2:1 internal resonance. In turn, by accounting for a multi-degree-of-freedom model, Koh and Rong (2004) showed a quantitative agreement of numerical

and experimental results as regards the dynamic tension responses of a non-resonant cable.

Herein, upon presenting the experimental cable model and setup (Sect. 2), the spectrum of natural frequencies of the system and the corresponding mode shapes are determined experimentally and verified numerically through a finite element discretization (Sect. 3). Then, in Section 4.1, based on the experimentally identified range of first frequency avoidance, frequency- and forcing amplitude-response diagrams are obtained in the relevant neighbourhood for several parametrically-excited inclined sagged cables. Because simultaneous primary external and internal resonances take place due to the commensurability of system in-plane and out-of-plane frequencies – thus entailing a principal parametric resonance – the occurrence of multi-mode responses is experimentally highlighted and its variable features in dependence of cable nearness to avoidance are discussed. In Section 4.2, the experimental outcomes are complemented with and qualitatively confirmed via numerical finite-difference simulations (Srinil and Rega, 2008) of the nonlinear partial-differential equations governing the 3-D dynamics of a parametrically excited cable, based on an exact kinematic description proposed and validated by Srinil *et al.* (2007). At the same time, further insight into the space-time varying histories of the parametrically-externally resonant dynamic displacement and tension is provided. The paper ends with some conclusions.

2. Experimental model and setup

A number of challenging tasks have to be tackled in designing the experimental apparatus and a reliable investigation of a flexible distributed-parameter system susceptible to undergo large-amplitude 3-D forced vibration, as is the case of a flexible sagged inclined cable.

Herein, in the background of a general theoretical 3-D modelling and energy-based formulation of the finite-amplitude dynamics of elastic suspended cables accounting for overall inertia effect and system asymmetry due to a sagged inclined configuration (Srinil *et al.*, 2007), a large-scale experimental setup and its testing apparatus are built up, as schematically displayed in Fig. 1 with end support details. A 30° inclined cable is considered, with the reference horizontal X_H and vertical Y_H span lengths equal to 3.03 and 1.75 m, respectively. The cable is a small-diameter, empty-filled surgical tubing, having the in situ values of mass per unit length equal to 0.0453 kg/m and net cross-section area equal to $5.8875 \times 10^{-5}\,\mathrm{m}^2$. The material is theoretically

assumed to be homogeneous and linearly elastic with estimated Young's modulus E equal to 1.225 MPa. In turn, the influence of torsion, shear, bending and temperature, somehow affecting cable dynamic responses, is disregarded.

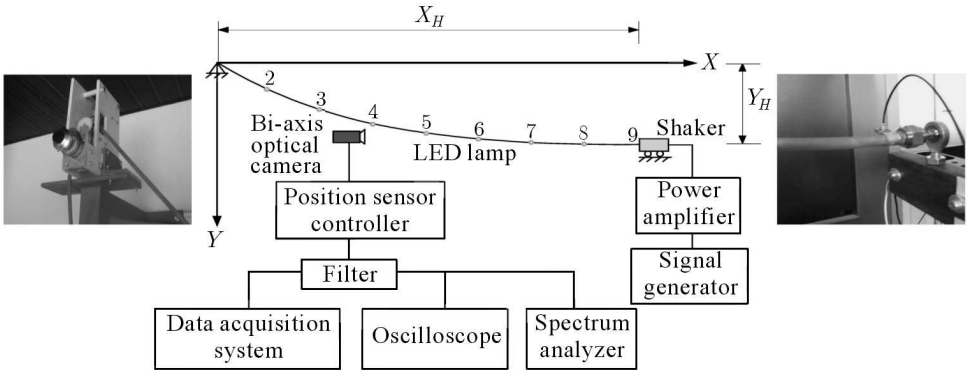

Fig. 1. Schematic view of cable model and experimental setup with support details

To carry out a measurement series of different sagged cables, the cable length – and thus cable sag – is varied (between 3.30-3.62 m) through the modified cogwheel at the upper pinned support. For convenience, the cable sag-to-span ratio at the middle span d_m (node No. 5) is considered as a geometrical control parameter, instead of the well-known elasto-geometric parameter λ/π (Triantafyllou and Grinfogel, 1986), due to lack of measured data of the variable deformed cable length and static tension. The lower cable end is fixed and pin-connected to the vibration shaker, which is mechanically kept stationary when undertaking linear dynamics and guided sliding in the cable horizontal direction when performing nonlinear dynamics. In the latter case, the shaker is harmonically driven via a power control unit (amplifier) and a function generator having a controllable frequency and gain. In both free and forced vibration tests, a bi-axis optical camera (Hamamatsu C7339) is utilized as a contact-free device measuring cable linear/nonlinear dynamic responses along two orthogonal (either horizontal/vertical or vertical/out-of-plane) directions according to the fixed Cartesian 3-D frame. A companion controller is implemented to digitally control and verify the positioning sensor of the camera, which detects the position of a spot emitting a continuous light. Upon several attempts, it has been found appropriate to illuminate the cable with a very light-weight LED (light emitting diode) operating with red color. Several LEDs are attached to the cable points horizontally equidistant from each other (nodes No. 2-8), all being necessary for modal shape identification. Measurements, observed via an oscilloscope and a spectrum analyser, are acquired by

a digital computer data acquisition system storing real time outputs at the sampling interval of 1/400 second with the frequency resolution of 0.002 Hz. A usual filter unit is implemented to cut off high frequencies induced by some overall noise. The recorded response is post-processed by means of the ARTeMIS extractor software (Structural Vibration Solutions Aps, 2002) and MATLAB. The gained data accuracy depends on a number of factors including, e.g., the imperfection of camera arrangements, the environmental temperature and disturbance. Unwanted effects are minimised by repeating several tests, which lead to the following optimised results.

3. Linear free vibration: frequency avoidance and hybrid modes

In the linear field, we experimentally aim (i) at constructing the natural frequency spectrum and (ii) at identifying the corresponding mode shapes of different sagged inclined cables, with also numerical finite element-based verifications.

From a standard free vibration test initiating the cable with small impulsive amplitudes, out-of-plane and in-plane frequencies are recorded by making use of one camera. Their values are estimated and non-dimensionalised with respect to the lowest out-of-plane frequency. Yet, to discriminate between the associated mode shapes, four cameras are contemporaneously used. Only in-plane modes with horizontal/vertical displacement components are identified, whereas out-of-plane modes can be visually observed for being similar to the taut-string eigenmodes. In circumventing the high modal density of inclined cable suspensions (Srinil and Rega, 2007b), at least two (or more) data sets having one (or more) reference point(s) are necessary to capture as many significant responses as desired. Here, three data sets are proposed, i.e., two data sets using four cameras/LEDs and another data set using three cameras/LEDs, all of them sharing two reference nodes (No. 3 and No. 6). Consequently, by gathering all of the acquired data, natural frequencies and corresponding modes are numerically evaluated based on the enhanced frequency domain decomposition and a technique (Structural Vibration Solutions Aps, 2002) accounting for proper orthogonal modes.

Figure 2 illustrates, versus the sag d_m, a comparison between experimental (circles) and numerical (catenary-based) finite element (Srinil *et al.*, 2007) (lines) results for the first three out-of-plane/in-plane normalised frequencies. 50 elements are used in the numerical solution. Experimental and numerical results are in good qualitative as well as quantitative agreement by exhibiting

the frequency avoidance of the first two in-plane modes ($0.14 < d_m < 0.16$). They also ensure the independence of out-of-plane frequencies on the sag parameter. The second frequency avoidance of higher-order in-plane modes seems to occur as well in a larger sag range. It is worth mentioning how, although the cable material is highly extensible (small E value), no first elastic frequency (Burgess and Triantafyllou, 1988) – with the relevant interactions – do occur at the considered low-order in-plane modes, which exhibit however nearly comparable horizontal and vertical displacement components, owing to cable inclination.

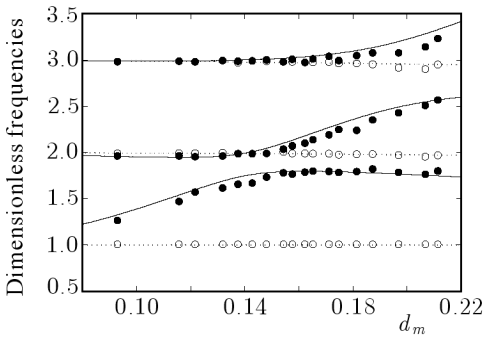

Fig. 2. A comparison of frequency avoidance phenomenon with numerical (lines) and experimental (circles) results: solid (dashed) lines and black (empty) circles denote in-plane (out-of-plane) dimensionless frequencies

Table 1. Comparison of experimental (EXP) and numerical finite element (FEM) results

Cable	d_m	Out-of-plane frequencies [Hz]				In-plane frequencies [Hz]			
		O1		O2		I1		I2	
		EXP	FEM	EXP	FEM	EXP	FEM	EXP	FEM
E1	0.093	1.10	1.04	2.17	2.08	1.38	1.38	2.11	2.04
E2	0.132	0.90	0.88	1.80	1.74	1.47	1.48	1.77	1.72
E3	0.154	0.84	0.81	1.68	1.61	1.48	1.45	1.72	1.70
E4	0.171	0.80	0.77	1.58	1.53	1.42	1.38	1.76	1.75

Table 1 compares some dimensional frequency values (in Hz) for different – shallower or slacker – extensible cables (E1-E4) being near (E2, E3) and away (E1, E4) from the avoidance in Fig. 2. Good quantitative agreement with small percent differences (less than 6%) is highlighted, showing also the similarity of experimental and FEM values of the first two in-plane frequencies irrespective

of the cable being near or far away from avoidance. Cable E3 experimentally seems to be the best nearly-tuned, internally 1:1 (I1:I2) resonant cable, whose spectral densities accounting for all data sets are exemplified in Fig. 3, which displays the frequency nearness at avoidance along with widely-spaced higher-order frequency contents.

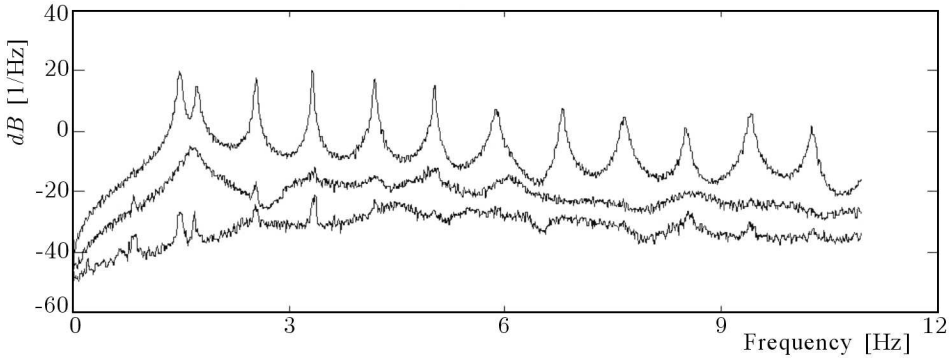

Fig. 3. Spectral densities associated with in-plane frequencies for cable E3

By focusing on the lowest four in-plane (I1-I4) frequencies, Fig. 4 compares experimental vs. numerical finite-element mode shapes of normalized horizontal/vertical displacements for cables E1, E3 and E4. Accuracy of experimental modal identifications is justified because of the good qualitative as well as quantitative correspondence in Fig. 4. Cable E1 exhibits nearly symmetric and anti-symmetric shapes of odd and even modes, respectively, owing to the low sag ($d_m = 0.093$). On the contrary, the asymmetry influences the modes – especially the hybrid ones (I1 and I2) coexisting near avoidance – for the larger-sagged ($d_m = 0.154$) cable E3, which, in turn, highlights comparable horizontal/vertical displacement amplitudes due to the inclination effect (Srinil and Rega, 2007b; Rega and Srinil, 2007). In this respect, the usual theoretical (so-called condensed) modelling ruling out the horizontal inertia is not recommended (Srinil and Rega, 2007a). It should be emphasised that a proper selection of cable reference points also plays an important role in the outcome of experimental – especially asymmetric – shapes. In any case, we suggest obtaining *a priori* theoretical modes of interest based on the general non-condensed model accounting for longitudinal inertia (Srinil *et al.*, 2007), and then determining the candidate points (unnecessarily being those at the mid- or quarter-span) where maximal or minimal amplitudes are possibly attained, the former being useful for mode classification and normalisation, whereas the latter allowing one to capture a nearly zero-deflection point where the mode shape changes curvature. In this study, referring to LEDs No. 3

and 6 provides good spatial identification of such measured in-plane modes for all of the considered cables.

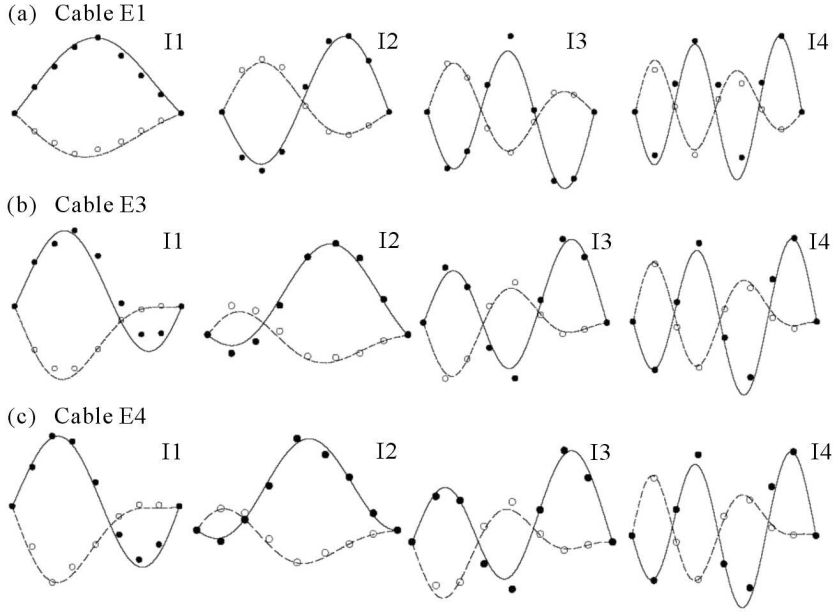

Fig. 4. Comparison of experimental (circles) and numerical finite element (lines) in-plane mode shapes: solid (dashed) lines and black (empty) circles denote vertical (horizontal) displacements

4. Nonlinear forced vibration: 3-D modal interaction due to parametric/external resonances

Considering an inclined cable subject to horizontally time-varying motion of the support with a given (sweeping) harmonic frequency Ω [Hz] and electric-force amplitude F (volts), we intend (i) to experimentally highlight the features of nonlinear modal interactions for near or away from avoidance cables (Fig. 2), and (ii) to complement experimental outcomes by some finite-difference simulations of the associated partial-differential equations governing kinematically exact 3-D cable motion (Srinil *et al.*, 2003; 2004).

4.1. Experimental results

In the large-amplitude regime of cable motion, steady-state vertical and out-of-plane dynamic responses are measured using one camera targeting LED

No. 2 (Fig. 1) for three re-installed cables E1, E3 and E4 (Table 1). Indeed, out-of-plane or in-plane motion of the other, generic or near-support, nodes is too large to be reliably detected by the optical cameras. Both frequency- and force-response diagrams are experimentally constructed with quasi-statically sweeping up and down analysis, in which the obtained amplitudes are numerically calibrated in volts through relevant peaks of estimated power spectra. In any experiment, the moving support amplitude ranges approximately in between 0-3 cm (varying F), and Ω is swept near the second in-plane I2 frequency (varying Ω), unless otherwise stated. Because of the high-dimensional space-time variability entailing multimodal responses, the nonlinear modes – and especially the in-plane asymmetric ones – are not experimentally identified. Yet, their profiles will be readily visualised via finite-difference outcomes.

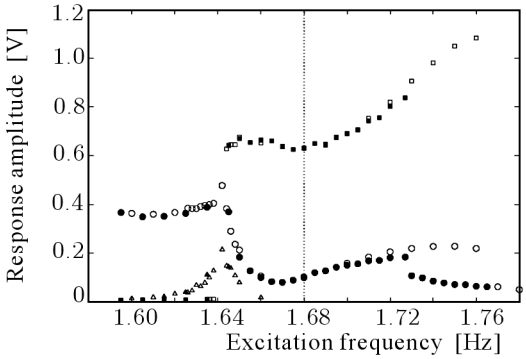

Fig. 5. Experimental frequency-response curves for cable E3 with frequency swept around I2 and $F = 0.8$ V: circle or triangle (square) denotes vertical (out-of-plane) amplitudes via sweeping-up (empty) and -down (filled) tests

Figure 5 depicts the frequency-response diagram for avoidance cable E3, which is considered as the best nearly-tuned planar 1:1 (I1:I2) resonant cable. Far away from the perfect primary external resonance of I2 mode ($\Omega = 1.72$), the cable response is actually planar and is dominated just by this mode (circles). However, over a large Ω range around the primary resonance, the dominant motion amplitude is seen to be non-planar due to the principal parametric resonance of lowest symmetric out-of-plane O1 mode, which is driven into the response according to a nearly-tuned 2:1 internal resonance between I2 ($\omega_{\mathrm{I2}} = 1.72$ Hz) and O1 ($\omega_{\mathrm{O1}} = 0.84$ Hz) modes (circles vs. squares). Formally, a combination of the primary external resonance ($\Omega = \omega_{\mathrm{I2}} + \sigma_{ex}$) and 2:1 internal resonance ($\omega_{\mathrm{I2}} = 2\omega_{\mathrm{O1}} + \sigma_{in}$) with σ_{ex} and σ_{in} representing external and internal detunings, respectively, entails activation of the principal parametric resonance ($\Omega = 2\omega_{\mathrm{O1}} + (\sigma_{in} + \sigma_{ex}) = 2\omega_{\mathrm{O1}} + \sigma_p$), with

σ_p being the ensuing parametric detuning. When sweeping Ω up and down, typical jump (hysteresis) phenomena take place along with pitchfork bifurcations resulting in overlapping of nonlinear dynamic responses and transitions from non-planar to planar responses and vice versa. In Fig. 5, simultaneous parametric/external resonances do occur, centered near $\Omega_p \approx 1.68$ Hz with a nearly-vanishing ($\sigma_{in} \approx 0.04$) internal detuning parameter of non-planar 2:1 resonance (Table 1).

Onset of spatial motion as the excitation frequency increases is also clearly highlighted by the experimental time histories of vertical (v) and out-of-plane (w) displacement components in Fig. 6. Left away from the primary resonance ($\Omega = 1.60$) the response is strictly planar (Fig. 6a), whereas multimodal interaction with the dominant out-of-plane response already occurs at $\Omega = 1.65$ (Fig. 6b), and nearly tuned, non-planar, 2:1 resonant interaction is full recognizable at $\Omega = 1.72$ and 1.76 (Fig. 6c,d).

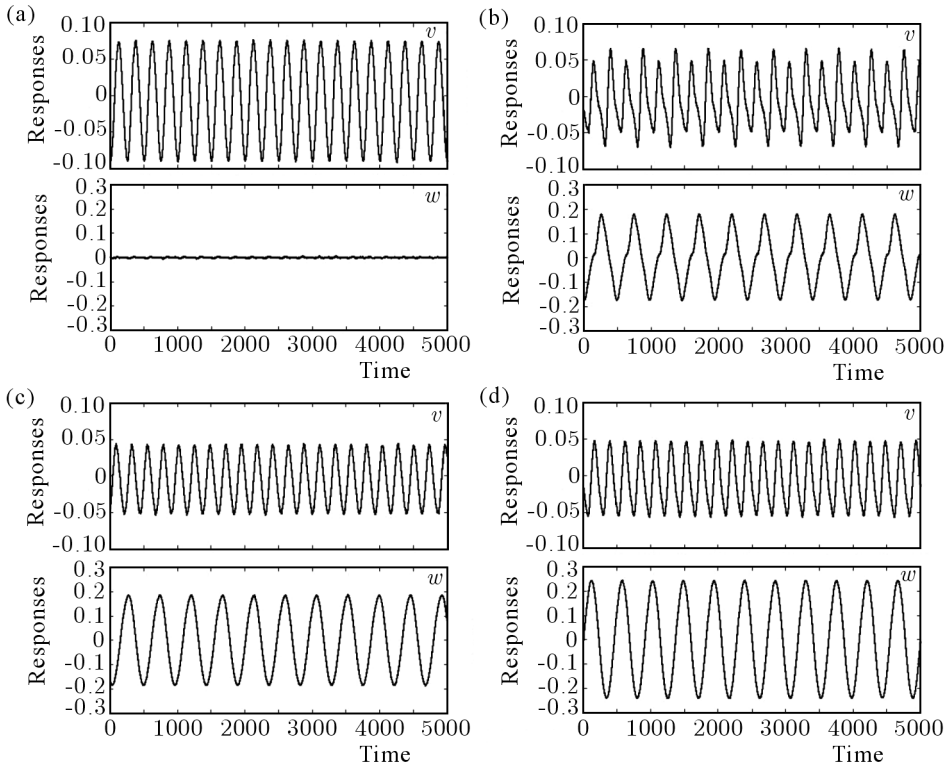

Fig. 6. Experimental time histories of steady-state vertical in-plane (v) and out-of-plane (w) responses for cable E3 under support motion amplitude equal to 0.8 V: (a) $\Omega = 1.60$; (b) $\Omega = 1.65$; (c) $\Omega = 1.72$; (d) $\Omega = 1.76$ Hz

Force-response diagrams of cable E3, obtained by sweeping F up and down, are reported in Fig. 7 for two different, though neighbouring, values of the excitation frequency within the range of activation of the principal parametric resonance. The planar response due to the pure primary resonance of I2 mode is seen to occur only for low excitation amplitudes, whereas the spatial response exhibiting the dominant parametrically excited out-of-plane component occurs over a large F range. At both values of the excitation frequency, coupled out-of-plane and in-plane amplitudes grow monotonously with increasing F, with no saturation phenomenon. Although catching details of bifurcation mechanisms is not an easy task in experimental analyses, for a lower excitation frequency (Fig. 7a) the out-of-plane component of the response seems to originate through a supercritical pitchfork bifurcation, whereas for the higher excitation frequency (Fig. 7b) the jump phenomena and the overlapping of unimodal (I2) and bimodal (I2-O1) responses attained for increasing and decreasing F, respectively, are likely to correspond to a subcritical pitchfork bifurcation of the out-of-plane response.

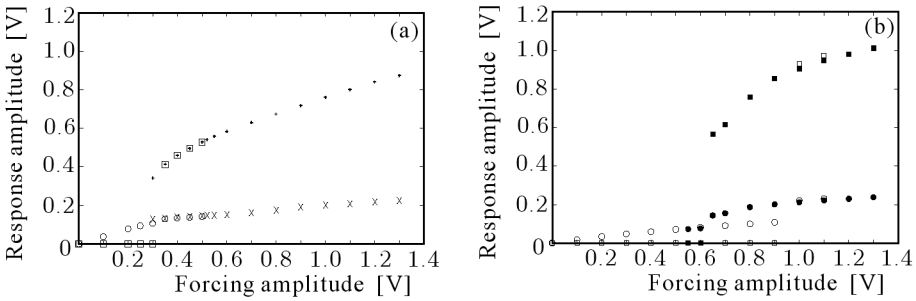

Fig. 7. Experimental forcing-response curves of cable E3 for (a) $\Omega = 1.71$ and (b) $\Omega = 1.74$ Hz: circle or triangle (square) denotes vertical (out-of-plane) amplitudes via sweeping-up (empty) and -down (filled) tests

Overall, the experimental results obtained for cable E3 exhibit comparable qualitative features to those of the theoretical results by Perkins (1992), where a tangential support excitation of a horizontal cable at the first crossover was considered. In particular, owing to the parametric resonance, Fig. 5 exhibits a typical asymmetric frequency-response diagram of 2:1 internal resonance with trivial (or nearly vanishing) internal detuning, whereas Fig. 7 exhibits both the typical – though different from each other – kinds of force-response diagrams observed by Perkins (1992) with vanishing or non-vanishing external detuning.

Herein, a major difference is that the associated planar spatial profiles at avoidance are asymmetric (hybrid) owing to the cable inclination effect. This

is likely to entail, e.g., the presence of small-amplitude responses of also fourth in-plane I4 mode (Fig. 4b) in Fig. 5 (triangles), where the non-planar resonance does not play any role (i.e. left to Ω_p). This kind of order-2 super-harmonic planar response arises because of a nearly-tuned 2:1 frequency ratio of I4 and I2 modes with relevant asymmetric modal shapes (Fig. 4b) being non-orthogonal (see the theoretical model in the background, Srinil and Rega (2007b)). This seems to be peculiar to the first avoidance inclined cable in comparison with the first crossover horizontal cable (Perkins, 1992), whose planar 2:1 resonance of I4 (anti-symmetric) and I2 (symmetric or anti-symmetric) modes cannot be activated due to nonlinear orthogonality properties (which entail vanishing interaction coefficients in the associated theoretical model, see Srinil and Rega (2007a)). Of course, I2-I4 modal interaction in the experimental inclined cable is seen to play a greater role when F is increased.

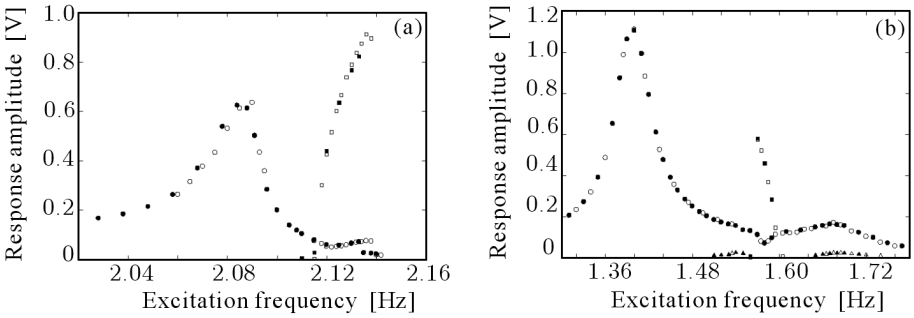

Fig. 8. Experimental frequency-response curves of cables (a) E1 ($F = 0.8\,\mathrm{V}$) and (b) E4 ($F = 0.5\,\mathrm{V}$): circle and triangle (square) denotes vertical (out-of-plane) amplitudes via sweeping-up (empty) and -down (filled) tests

Considering inclined cables E1 and E4 (Fig. 8a and 8b), which are far-away from avoidance, allows us to highlight the influence on parametrically-excited responses of either increasing or decreasing internal detuning. In Table 1, the two cables are seen to have experimental I2:O1 frequency ratio equal to 1.92 (E1) and 2.20 (E4) with respect to 2.05 value of cable E3, apart from different modal shapes (Fig. 4). In contrast to Figs. 5 (E3) and 8a (E1), a lower excitation amplitude ($F = 0.5\,\mathrm{V}$) is considered in Fig. 8b (E4) because of the parametric resonance being complemented by the already large response of I1 mode. By sweeping Ω, the regions of the principal parametric resonance (where the out-of-plane mode coexists with the in-plane one) and of the primary external resonance near I2 frequency are decoupled (i.e., separated from each other) in both Fig. 8a and Fig. 8b, with respect to Fig. 5. In Fig. 8a (8b), the parametric resonance is seen to occur in a narrow frequency band

right (left) to the primary resonance region, which is centered at $\Omega \approx 2.08$ (1.68) Hz instead of the initially measured value 2.11 (1.76) Hz (Table 1) due to the re-configuring process slightly affecting the basic properties of re-tested cables. As already said, Fig. 8b also highlights the primary resonant response of I1 mode (with the frequency centered at ≈ 1.40 Hz) whose amplitudes (LED No. 2) are greater than those due to the parametric (primary) resonance of O1 (I2) frequency. Of course, this is highlighted depending on the measured cable node, herein suitably chosen.

Again, the observed experimental nonlinear dynamics and interactions far away from avoidance are apparently in qualitative agreement with the theoretical results for the horizontal cable around the crossover with significant non-trivial values of the internal detuning parameter (Perkins, 1992). Indeed, Fig. 8a, whose non-trivial negative internal detuning ($\sigma_{in} \approx -0.12$) corresponds to the positive one in Perkins (1992), highlights an enhanced right-sided non-planar response qualitatively similar to that in Fig. 7a of that reference, whereas Fig. 8b, with its (lower) positive internal detuning ($\sigma_{in} \approx 0.08$) and its left-sided non-planar response, somehow corresponds to Fig. 7b therein. However, further distinguishing features also occur herein, still associated with the different role played in the two cases by the planar spatial profiles. In the horizontal cable, where the planar mode involved in 2:1 internal resonance at the crossover is the symmetric one, the regions of external and parametric resonances decouple (with somehow mirrored features left and right of the crossover) because of the symmetric mode being no more internally resonant with the (symmetric) out-of-plane mode. By contrast, in the inclined cable, where one of the two hybrid modes at avoidance (i.e., I2) is the planar mode (more directly) involved in 2:1 internal resonance, the decoupling occurs when moving to the left (cable E1, Fig. 8a) because of formerly hybrid I2 mode becoming nearly anti-symmetric (Fig. 4a), namely orthogonal to O1, though still being potentially 2:1 resonant with it. In turn, when moving to the right (cable E4, Fig. 8b), the right-sided decoupling of the non-planar response – as the one in Fig. 8a for cable E1 – is observed with respect to the external resonance region of the other (formerly hybrid at avoidance) planar I1 mode. Indeed, I1 is now playing the decoupling role of a nearly anti-symmetric, orthogonal mode (Fig. 4c) somehow comparable to that of I2 for cable E1, with its own internal detuning against potentially 2:1 resonant mode O1 being still negative ($\sigma_{in} = \omega_{\mathrm{I1}} - 2\omega_{\mathrm{O1}} \approx 1.42 - 1.60 = -0.18$) greater than that of cable E1 and such to entail a major separation of the external and parametric regions, though being cable E4 closer to avoidance than cable E1.

Overall, consistent with the theoretical predictions, the non-planar nonlinear interaction for cables away from avoidance is seen to be considerably weaker than for cables at nearly avoidance (Rega and Srinil, 2007), due to the major role played in the latter case by modal hybridity (non-orthogonality). Moreover, at avoidance, no interaction of the first hybrid mode I1 with the out-of-plane mode O1 is observed – due to barely tuned 2:1 resonance – even if the corresponding interaction coefficient in the underlying theoretical model is different from zero due to cable inclination (Srinil and Rega, 2007b). Yet, with respect to the crossover horizontal cable, whose non-planar 2:1 resonance is quite a localised phenomenon due to a strictly symmetric shape of the involved in-plane mode, the avoidance inclined cable is likely to exhibit a slightly larger zone of non-planar parametric resonance owing to persisting involvement of one of the coexisting hybrid modes whose shapes maintain a certain degree of spatial symmetry. In addition, the presence of higher-mode responses due to planar 2:1 resonance, though with small amplitudes, seems to be peculiar for avoidance cables as the nonlinear orthogonality of modes never holds due to the effect of cable inclination and sag.

4.2. Theoretical model and finite-difference results

The observed experimental 3-D responses due to the activation of non-planar internal resonance are now numerically verified with reference to a general theoretical model (Fig.1) of arbitrarily inclined cables. Based on an exact kinematical description of cable element, the nonlinear partial-differential equations governing the 3-D forced cable vibration, in dimensional form, read (Srinil *et al.*, 2007)

$$\begin{aligned}
&\Big(\frac{EA+EA(1+e_o)u'}{\sqrt{1+{y_o'}^2}}-\frac{EA(1+u')}{\sqrt{(1+u')^2+(y_o'+v')^2+{w'}^2}}\Big)'=\\
&\quad=\Big(\frac{w_C}{g}\ddot{u}+c_u\dot{u}\Big)\frac{\sqrt{1+{y_o'}^2}}{1+e_o}-F_u\sqrt{1+{y_o'}^2}\\
&\Big(\frac{EAy_o'+EA(1+e_o)v'}{\sqrt{1+{y_o'}^2}}-\frac{EA(y_o'+v')}{\sqrt{(1+u')^2+(y_o'+v')^2+{w'}^2}}\Big)'=\\
&\quad=\Big(\frac{w_C}{g}\ddot{v}+c_v\dot{v}\Big)\frac{\sqrt{1+{y_o'}^2}}{1+e_o}-F_v\sqrt{1+{y_o'}^2}
\end{aligned}\tag{4.1}$$

$$\Big(\frac{EA(1+e_o)w'}{\sqrt{1+y_o'^2}} - \frac{EAw'}{\sqrt{(1+u')^2+(y_o'+v')^2+w'^2}}\Big)' =$$
$$= \Big(\frac{w_C}{g}\ddot{w} + c_w\dot{w}\Big)\frac{\sqrt{1+y_o'^2}}{1+e_o} - F_w\sqrt{1+y_o'^2}$$

where $u(x,t)$, $v(x,t)$, $w(x,t)$ are the dynamic horizontal, vertical and out-of-plane displacement components in a Cartesian coordinate frame XYZ measured from the static equilibrium configuration $y_o(x)$ attained by the cable under its own gravity g, e_o is the initial static strain, E, A and w_C are cable Young's modulus, cross-sectional area and self-weight per unit unstretched length, respectively, and c_u, c_v, c_w are viscous damping coefficients. A prime (dot) represents partial differentiation with respect to the horizontal space coordinate x (time t). The distributed external forcing (F_i) terms are assumed to be trivial in this study as we neglect the effect that might result from other sources of spatial excitation. As in the experimental case, we focus on the problem of right-support horizontal excitation whose boundary conditions read

$$\begin{aligned} &u(0,t) = v(0,t) = w(0,t) = v(X_H,t) = w(X_H,t) = 0 \\ &u(X_H,t) = u_0\cos\Omega t \end{aligned} \tag{4.2}$$

Here, u_0 is a constant amplitude of the support motion. Space-time numerical simulation of Eqs (4.1) and (4.2) is carried out via a second-order finite-difference approach centrally approximating both spatial and temporal derivatives, thanks to a straightforward routine (Srinil *et al.*, 2003, 2004) employing hybrid explicit-implicit numerical integration along with a predictor-corrector implementation. This approach has recently been validated against a multiple scales solution by Srinil and Rega (2008).

Being interested in a qualitative confirmation of the activation of the non-planar parametric resonance in proper excitation conditions, cable E3 with $u_0 = 2\,\text{cm}$ and $\Omega \approx 1.70\,\text{Hz}$ (Fig. 5) is considered. Since only rough estimates of the actual viscous damping values have been obtained in the experiment, we use the formula $c = 2\xi\sqrt{EA\rho}$ (Koh and Rong, 2004), where ρ is the cable density (i.e., $\rho = w_C/Ag$), by first assuming a damping ratio $\xi = 1\%$ for the in-plane response and no damping for the out-of-plane response. 30 cable segments and a time-step equal to $10^{-5}\,\text{s}$ are accounted for. To avoid long transients preceding the onset of the parametric resonance, lowest symmetric out-of-plane spatial initiations with small amplitudes are assigned, along with zero in-plane initiations.

Nonlinear time histories of the horizontal/vertical (out-of-plane) amplitudes (normalized with respect to X_H) at LED No. 2 (Fig. 1) are plotted in Fig. 9a (b), whereas the corresponding total tension (normalized with respect to the maximum static tension) responses – which are space-time dependent according to the adopted general non-condensed model (Rega and Srinil, 2007) – are shown in Fig. 9c. The horizontal (vertical) vs. out-of-plane displacement projections at the mid-span are traced out in the phase portrait of Fig. 9d. Overall, Figs. 9a-d highlight two successive portions of the system resonant response, a transient one ($T < 70$) consisting of solely primary external planar motion (with negligible out-of-plane component), and a steady one ($T > 70$) highlighting the occurrence of a principal parametric/external spatial response (with dominant out-of-plane component), along with considerable positive and negative planar drifts for the horizontal and vertical components, respectively (Fig. 9a,d). Such space-dependent drifts are associated with system quadratic nonlinearities (Srinil *et al.*, 2007b).

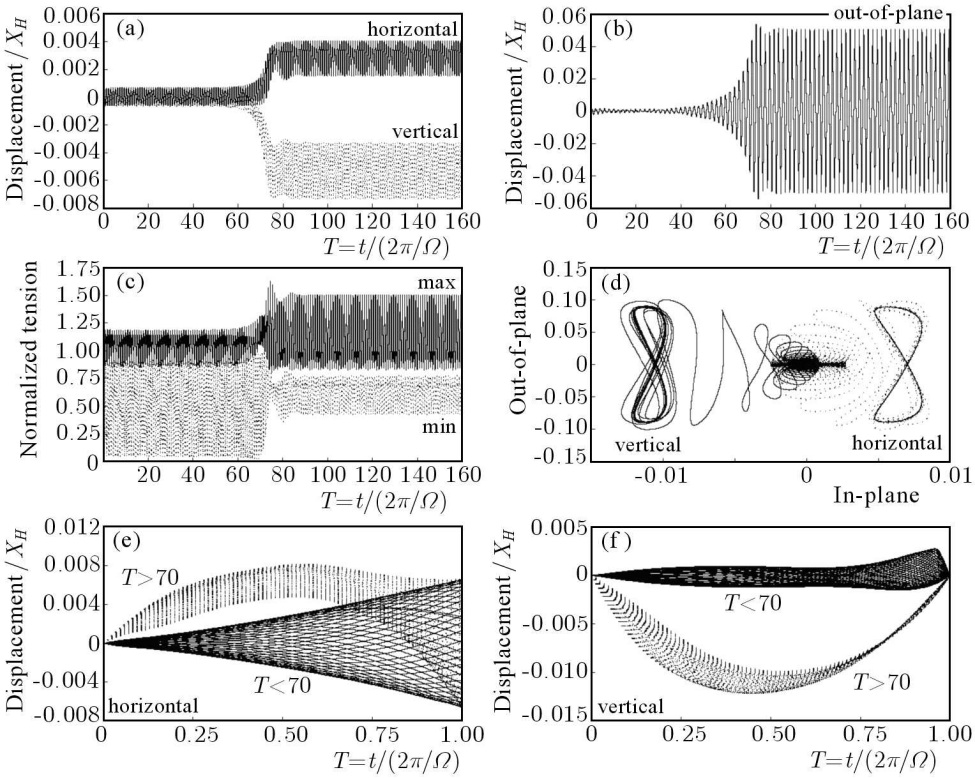

Fig. 9. Space-time numerical simulations for the parametrically excited inclined cable E3

While qualitatively confirming the experimentally observed activation of simultaneous parametrically-externally resonant dynamics for cable E3, numerical results also furnish further insights into interesting features of the system response, such as the varied maximum and minimum tension due to parametric/external vs. primary resonances (Fig. 9c), and typical 2:1 internally resonant figure "eight" (vertical and horizontal) trajectories in the corresponding phase portraits (Fig. 9d). Moreover, the spanwise distributions of time-varying horizontal (vertical) displacements are visualized in Fig. 9e (f), distinguishing between the initial primary (solid) and the successive parametric/external (dotted) resonant profiles. The parametric resonance of symmetric out-of-plane motion greatly affects the in-plane responses which, in turn, exhibit strong spatial asymmetry due to both the one-end support excitation and the cable inclination effect.

It is also worth noting how the qualitative features of the cable response are strongly sensitive to a small damping variation in numerical simulations. Indeed, when considering a non-vanishing (even small) damping ratio for the out-of-plane response, in addition to the in-plane one, no parametrically non-planar resonance is numerically observed. Therefore, careful estimation of damping parameters is one of the crucial aspects in the experiment and deserves further investigation.

5. Conclusions

Experimental studies on free and parametrically-forced vibrations of sagged inclined cables have been carried out and discussed against theoretical and numerical analyses. For the linear free vibration, the systematic experimental approach provides worthwhile confirmation of the frequency avoidance phenomenon and associated hybrid (mixed symmetric/anti-symmetric) modes of horizontal/vertical displacements. The nonlinear dynamical problem of harmonically time-varying support movement has been considered by focusing on inclined cables in the neighbourhood of first avoidance. Experimental results for the near-avoidance cable highlight typical frequency- and force-response diagrams involving non-planar interactions of 2:1 resonant in-plane/out-of-plane (hybrid/symmetric) modes due to simultaneous primary external and principal parametric (external plus internal) resonances with possible involvement of also a higher-order in-plane mode due to planar 2:1 resonance. On the contrary, decoupling of the regions of external and parametric resonance is observed for cables farther away from avoidance. The role played in nonlinear

responses of inclined cables by their varying modal hybridity near the first avoidance is discussed also in the background of companion literature results for horizontal cables near the first crossover.

By referring to a general 3-D inclined cable model based on exact kinematics, a companion description of out-of-plane/in-plane nonlinear dynamics for the parametrically excited system is achieved through direct finite-difference simulation of the corresponding nonlinear partial-differential equations of motion. Numerical results complement the experiments as regards features of primary external vs. parametric/external excitations and the associated transition, total tension time histories and spatio-temporal displacement distributions, which allow us to draw the meaningful issue of cable asymmetry induced by the actual sagged inclined configuration.

Acknowledgements

The authors gratefully acknowledge the support of the Sapienza University of Rome through the Ricerche d'Ateneo programme, and the dynamical laboratory facilities of the University of L'Aquila.

References

1. Alaggio R., Rega G., 2000, Characterizing bifurcations and classes of motion in the transition to chaos through 3D-tori of a continuous experimental system in solid mechanics, *Physica D*, **137**, 70-93
2. Benedettini F., Rega G., 1997, Experimental investigation of the nonlinear response of a hanging cable. Part II: Global analysis, *Nonlinear Dynamics*, **14**, 119-138
3. Burgess J.J., Triantafyllou M.S., 1988, The elastic frequencies of cables, *Journal of Sound and Vibration*, **120**, 153-165
4. Cheng S.P., Perkins N.C., 1994, Theoretical and experimental analysis of the forced response of sagged cable/mass suspensions, *ASME Journal of Applied Mechanics*, **61**, 944-948
5. Ibrahim R.A., 2004, Nonlinear dynamics of suspended cables. Part III: Random excitation and interaction with fluid flow, *ASME Applied Mechanics Reviews*, **57**, 515-549
6. Irvine H.M., 1981, *Cable Structures*, MIT Press, Cambridge, MA
7. Irvine H.M., Caughey T.K., 1974, The linear theory of free vibrations of a suspended cable, *Proceedings of the Royal Society London*, **A 341**, 299-315

8. Koh C.G., Rong Y., 2004, Dynamic analysis of large displacement cable motion with experimental verification, *Journal of Sound and Vibration*, **272**, 187-206

9. Lee C.L., Perkins N.C., 1993, Experimental investigation of isolated and simultaneous internal resonances in suspended cables, In: *Nonlinear Vibrations*, Ibrahim R.A., Bajaj A.K., Bergman L.A. (Eds), *ASME*, DE-**54**, 21-31

10. Perkins N.C., 1992, Modal interactions in the non-linear response of elastic cables under parametric/external excitation, *International Journal of Non-linear Mechanics*, **27**, 233-250

11. Rega G., 2004, Nonlinear dynamics of suspended cables, Part I: Modeling and analysis; Part II: Deterministic phenomena, *ASME Applied Mechanics Reviews*, **57**, 443-514

12. Rega G., Alaggio R., Benedettini F., 1997, Experimental investigation of the nonlinear response of a hanging cable. Part I: Local analysis, *Nonlinear Dynamics*, **14**, 89-117

13. Rega G., Srinil N., 2007, Nonlinear hybrid-mode resonant forced oscillations of sagged inclined cables at avoidances, *ASME Journal of Computational and Nonlinear Dynamics*, **2**, 324-336

14. Russell J.C., Lardner T.J., 1998, Experimental determination of frequencies and tension for elastic cables, *ASCE Journal of Engineering Mechanics*, **124**, 1067-1072

15. Srinil N., Rega G., 2007a, The effects of kinematic condensation on internally resonant forced vibrations of shallow horizontal cables, *International Journal of Non-Linear Mechanics*, **42**, 180-195

16. Srinil N., Rega G., 2007b, Two-to-one resonant multi-modal dynamics of horizontal/inclined cables, Part II: Internal resonance activation, reduced-order models and nonlinear normal modes, *Nonlinear Dynamics*, **48**, 253-274

17. Srinil N., Rega G., 2008, Space-time numerical simulation and validation of analytical predictions for nonlinear forced dynamics of suspended cables, *Journal of Sound and Vibration*, **315**, 394-413

18. Srinil N., Rega G., Chucheepsakul S., 2003, Large amplitude three-dimensional free vibrations of inclined sagged elastic cables, *Nonlinear Dynamics*, **33**, 129-154

19. Srinil N., Rega G., Chucheepsakul S., 2004, Three-dimensional nonlinear coupling and dynamic tension in the large amplitude free vibrations of arbitrarily sagged cables, *Journal of Sound and Vibration*, **269**, 823-852

20. Srinil N., Rega G., Chucheepsakul S., 2007, Two-to-one resonant multi-modal dynamics of horizontal/inclined cables, Part I: Theoretical formulation and model validation, *Nonlinear Dynamics*, **48**, 231-252

21. Structural Vibration Solution Aps, 2002, ARTeMIS Extractor Software Version 3.2, NOVI Science Park, Niels Jernes Vej 10, Aalborg East, Denmark

22. Triantafyllou M.S., 1984, Linear dynamics of cables and chains, *Shock and Vibration Digest*, **16**, 9-17

23. Triantafyllou M.S., 1987, Dynamics of cables and chains, *Shock and Vibration Digest*, **19**, 3-5

24. Triantafyllou M.S., 1991, Dynamics of cables, towing cables and mooring systems, *Shock and Vibration Digest*, **23**, 3-8

25. Triantafyllou M.S., Grinfogel L., 1986, Natural frequencies and modes of inclined cables, *ASCE Journal of Structural Engineering*, **112**, 139-148

26. Xu Y.L., Zhan S., Ko J.M., Yu Z., 1999, Experimental study of vibration mitigation of bridge stay cables, *ASCE Journal of Structural Engineering*, **125**, 977-986

Doświadczalne i numeryczne badania obciążonych lin ukośnych: drgania swobodne i wymuszone parametrycznie

Streszczenie

Ubogie opracowania literaturowe dotyczące badań eksperymentalnych ukośnych lin przenoszących obciążenie skłoniły autorów tej pracy do zajęcia się problemem modelowania liniowych i nieliniowych drgań ugiętych lin ukośnych w oparciu o dyskusję otrzymanych wyników badań teoretycznych i numerycznych. Uwagę skoncentrowano na identyfikacji hybrydowych postaci drgań własnych lin wywołanych asymetrią, która prowadzi do tzw. zjawiska unikania częstości dającego się zaobserwować w spektrum układu. Dokonano analizy trójwymiarowego układu z uwzględnieniem jednoczesnego działania parametrycznego/zewnętrznego wymuszenia ruchem harmonicznym punktu zamocowania liny. Wielomodalne płaskie i niepłaskie wzajemne oddziaływania o dużej amplitudzie wywołane płaskimi i niepłaskimi rezonansami wewnętrznymi potwierdzono doświadczalnie i przewidziano w drodze symulacji numerycznych cząstkowych różniczkowych równań ruchu liny z nieliniowością geometryczną przy wzbudzeniu parametrycznym. Otrzymane rezultaty badań doświadczalnych i numerycznych uwypukliły charakterystyczne cechy liniowej/nieliniowej dynamiki lin ukośnych ze szczególnym podkreśleniem roli asymetrii w układzie spowodowanej niezerowym kątem nachylenia liny, towarzyszącej pozostałym efektom, takim jak zwis i dynamiczna rozszerzalność.

Manuscript received January 18, 2008; accepted for print January 31, 2008